RESEARCH ARTICLE

NANO · MICRO small
www.small-journal.com

Grinding-Induced Water Solubility Exhibited by Mechanochromic Luminescent Supramolecular Fibers

*Qiming Liu, Tianyue Zhang, Yuka Ikemoto, Yudai Shinozaki, Go Watanabe, Yuta Hori, Yasuteru Shigeta, Takemi Midorikawa, Koji Harano, and Yoshimitsu Sagara**

Most mechanochromic luminescent compounds are crystalline and highly hydrophobic; however, mechanochromic luminescent molecular assemblies comprising amphiphilic molecules have rarely been explored. This study investigated mechanochromic luminescent supramolecular fibers composed of dumbbell-shaped 9,10-bis(phenylethynyl)anthracene-based amphiphiles without any tetraethylene glycol (TEG) substituents or with two TEG substituents. Both amphiphiles formed water-insoluble supramolecular fibers via linear hydrogen bond formation. Both compounds acquired water solubility when solid samples composed of supramolecular fibers are ground. Grinding induces the conversion of 1D supramolecular fibers into micellar assemblies where fluorophores can form excimers, thereby resulting in a large redshift in the fluorescence spectra. Excimer emission from the ground amphiphile without TEG chains is retained after dissolution in water. The micelles are stable in water because hydrophilic dendrons surround the hydrophobic luminophores. By contrast, when water is added to a ground amphiphile having TEG substituents, fragmented supramolecular fibers with the same molecular arrangement as the initial supramolecular fibers are observed, because fragmented fibers are thermodynamically preferable to micelles as the hydrophobic arrays of fluorophores are covered with hydrophilic TEG chains. This leads to the recovery of the initial fluorescent properties for the latter amphiphile. These supramolecular fibers can be used as practical mechanosensors to detect forces at the mesoscale.

1. Introduction

Over the past 20 years, a vast number of organic compounds and organometallic complexes capable of changing their luminescence properties in response to mechanical stimuli have been developed owing to their potential applications in sensors and memory.[1–7] In most cases, the observed changes in luminescence properties were not caused by the force-induced cleavage of covalent bonds within the compound. Rather, they result from alterations in the molecular assembly, which is formed by the combination of various intermolecular interactions, such as hydrogen bonds, π-stacking, hydrophobic effect, and dipole–dipole interaction. Mechanochromic luminescent materials are ideal for detecting forces applied to hydrophobic materials, such as glass, metals, and polymers, as well as for detecting and visualizing the forces applied to or generated by living cells and other biomaterials. However, most reported organic[8–37] or organometallic[38–46] compounds cannot be utilized for the latter purpose because of their high crystallinity and/or hydrophobic molecular

Q. Liu, T. Zhang, Y. Sagara
Department of Materials Science and Engineering
Tokyo Institute of Technology
2-12-1 Ookayama, Meguro-ku, Tokyo 152–8552, Japan
E-mail: sagara.y.aa@m.titech.ac.jp

Y. Ikemoto
Japan Synchrotron Radiation Research Institute/SPring-8
1-1-1 Kouto, Sayo-cho, Sayo-gun, Hyogo 679–5198, Japan

Y. Shinozaki, G. Watanabe
Department of Physics
School of Science
Kitasato University
1-15-1 Kitazato, Minami-ku, Sagamihara, Kanagawa 252–0373, Japan

The ORCID identification number(s) for the author(s) of this article can be found under https://doi.org/10.1002/smll.202400063

DOI: 10.1002/smll.202400063

G. Watanabe
Department of Data Science
School of Frontier Engineering
Kitasato University
1-15-1 Kitazato, Minami-ku, Sagamihara, Kanagawa 252–0373, Japan

G. Watanabe
Kanagawa Institute of Industrial Science and Technology (KISTEC)
705–1 Shimoimaizumi, Ebina, Kanagawa 243–0435, Japan

Y. Hori, Y. Shigeta
Center for Computational Sciences
University of Tsukuba
1-1-1 Tennodai, Tsukuba, Ibaraki 305–8577, Japan

T. Midorikawa, K. Harano
Center for Basic Research on Materials
National Institute for Materials Science
1-1 Namiki, Tsukuba, Ibaraki 305-0044, Japan

K. Harano, Y. Sagara
Living Systems Materialogy (LiSM) Research Group
International Research Frontiers Initiative (IRFI)
Tokyo Institute of Technology
4259 Nagatsuda-cho, Midori-ku, Yokohama, Kanagawa 226–8503, Japan

structures. Moreover, compounds with hydrophilic molecular structures are highly limited[47–53] compared with hydrophobic mechanochromic luminescent compounds, which have been widely developed. Though a number of amphiphiles are known to form a variety types of molecular assembled structures including micelles, cylindrical micelles, vesicles, and planer membranes,[54–59] their mechanoresponsiveness has not been well investigated.

One challenge in utilizing mechanochromic fluorescent materials as practical mechanosensors is achieving quantification. Many existing crystalline materials have yet to address this issue. Crystalline materials, comprising numerous micro- and nanocrystals, exhibit a wide range of particle sizes. Consequently, the forces required to induce changes in molecular assembly differ; larger crystals need significant force to break, while smaller crystals can be broken with considerably less force. Additionally, due to their composition of a large number of molecules, crystalline compounds require a relatively large force to induce changes in luminescence properties. This characteristic of crystalline compounds spoils the advantage of mechanochromic materials based on alterations in molecular arrangement, which can elicit changes in luminescence properties with inherently weaker forces, as there is no need to break covalent bonds. Addressing these inherent issues in practical applications requires the construction of molecular assemblies that exhibit mechanochromic fluorescent properties with a uniform and limited number of molecules. Rather than constructing 3D molecular assemblies comprising a vast number of molecules, a low-dimensional molecular assembly should be pursued to detect very small forces and maintain uniform thresholds. Potential molecular assemblies include micelle-like aggregates with uniform size, 1D supramolecular fibers, and 2D molecular sheets of uniform thickness.

In 2014, a study reported that mechanochromic fluorescent micelles change their fluorescent color upon mechanical stimulation in water; these micelles were composed of 10–15 dumbbell-shaped amphiphiles.[50] In brief, 1,6-bis(phenylethynyl)pyrene was introduced as a luminescent group at the center of the amphiphile. Hydrophilic dendrons with multiple hydroxyl and amino groups at the periphery were attached to the luminophore via amide groups. In water, the amphiphile self-assembled into micelles, in which hydrogen bonds formed between the amide groups, and the fluorescent cores π-stacked to form a static excimer. Note that when micelles are loaded onto glass or polymer beads using commercially available crosslinkers, and sufficient force is applied, the arrangement of the luminophores changes, thus preventing them from forming excimers. This conversion results in a blueshift in the fluorescence spectrum. Because the micelles have almost the same size, a threshold of force exists to induce a change in the fluorescence color from yellow to green, which is suitable for practical mechanosensors. However, to induce the fluorescence color change in the micelles, all π-stacked arrangements of fluorophores must be changed into an arrangement that does not contain any excimers. If an excimer site exists, energy transfer occurs from other monomer-like regions, thus resulting in excimer-dominant fluorescence. Consequently, the sensitivity of the micelles is poor to mechanical stimuli.

To address these issues, this study investigated two mechanochromic supramolecular fibers consisting of amphiphiles with different hydrophilicities (**Figure 1**). Further, mechanical grinding endows the amphiphiles with water solubility owing to the transformation of their molecular assemblies. To the best of our knowledge, this is the first report of force-induced water solubility, accompanied by mechanochromic luminescence. The supramolecular fibers consisted of dumbbell-shaped amphiphiles based on 9,10-bis(phenylethynyl)anthracene, without or with tetraethylene glycol (TEG) chains on the fluorophore (Figure 1a). The present supramolecular fibers exhibited a grinding-induced redshift of the emission spectra, which is opposite to the blueshift observed in the emission of previously reported micelles.[50] The initial supramolecular fibers did not exhibit excimer fluorescence. By grinding in the solid states, the molecular assembly structures of the 1D fiber were converted to micellar structures, and the emitters formed excimers, thus causing the red shift of emission. Note that if even one excimer forms at any location within the 1D fibers, energy transfer occurs from the monomer-like fluorophores in the vicinity, thus leading to excimer-dominant fluorescence. Consequently, the sensitivity of the fiber far exceeded those of previous mechanochromic luminescent micelles. After the addition of water to the ground samples of amphiphiles without and with TEG chains, both samples became water-soluble, and different responses were observed (Figure 1b). In the former, without TEG groups, the excimer fluorescence was maintained in water because the micellar structures were stable and retained in water. By contrast, the latter, with TEG groups, recovered their initial fluorescent properties through conversion from thermodynamically unfavorable micellar structures to stable fragmented fibers. Given that such mechanochromic supramolecular fibers possess a width equivalent to that of a single molecule, they could serve as practical mechanosensing fluorescent materials if uniformly dispersed onto other materials. The fluorescence color would change upon the application of a force exceeding a certain threshold, with the magnitude of this force being very small.

Recently, supramolecular mechanophores capable of detecting pN-order forces at the single-molecule level were developed.[60–68] However, to use these mechanophores as molecular tools for detecting forces at the mesoscale level, they need to be introduced into polymers or supported on the surfaces of other materials. By contrast, the supramolecular fibers developed in this study are continuous molecular aggregates with lengths in the order of micrometers and can be used as is in mesoscale, which is highly advantageous.

2. Results and Discussion

The molecular structures of the 9,10-bis(phenylethynyl)anthracene derivatives **1** and **2** are shown in Figure 1. Two hydrophilic dendritic structures with twelve hydroxy groups at the peripheral positions were introduced into the fluorophore through amide groups to form hydrogen bonds in the molecular assemblies. Given that the fluorophore is hydrophobic, dumbbell-shaped compounds **1** and **2** are amphiphiles. In addition, two TEG chains were introduced to the fluorophore of **2** to enhance its hydrophilicity. Reportedly, several dumbbell-shaped amphiphiles exhibit mechanochromic luminescence.[48,50,51] A dumbbell-shaped pyrene derivative with

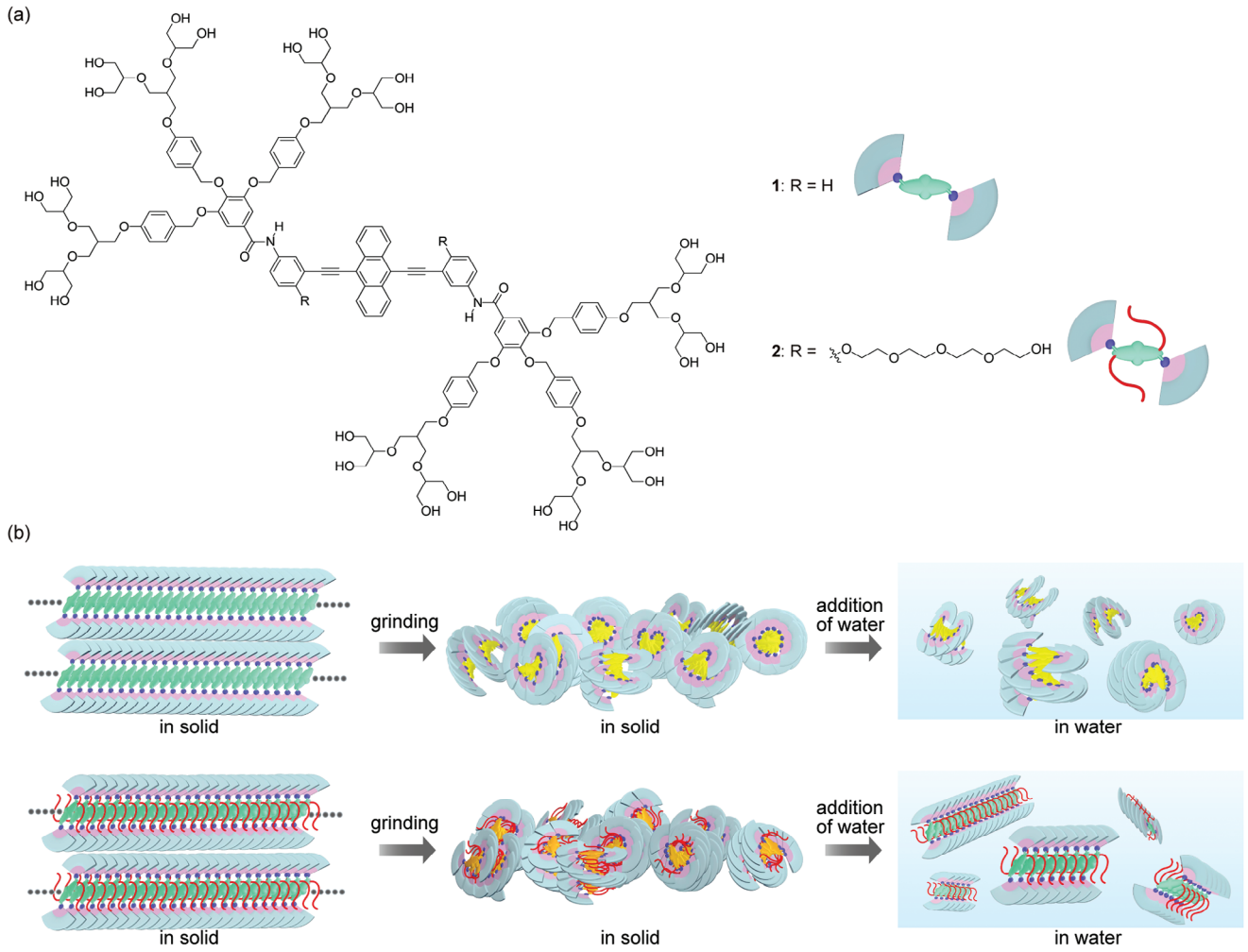

Figure 1. a) Molecular structures of amphiphiles **1** and **2**, along with schematics of each amphiphile. b) Schematic of the external stimuli-induced change in the molecular assembly of mechanochromic luminescence supramolecular fibers consisting of amphiphiles **1** (top) or **2** (bottom).

two bulky water-soluble dendritic structures was reported to exhibit reversible fluorescent color changes upon mechanical stimulation and exposure to water vapor in the solid phase.[48] Additionally, a pyrene derivative with reduced dendron bulkiness reportedly forms mechanochromic luminescent micelles.[50] For these dumbbell-shaped amphiphiles, dendrons were introduced along the long axis of the fluorophore. By contrast, for compounds **1** and **2**, the substitution positions of the dendrons are tilted 60° from the long axis of the luminophore, thereby resulting in a sheared, dumbbell-like molecular structure. These amphiphiles were expected to enable access to thermodynamically stable molecular assemblies other than micelles. Amphiphiles **1** and **2** were synthesized via Sonogashira coupling between 9,10-diiodoanthracene and dendritic groups in which all twelve hydroxyl groups were protected with triisopropylsilyl (TIPS) groups; subsequently, the TIPS groups were deprotected. Both **1** and **2** were characterized by ^{1}H and ^{13}C NMR spectroscopy and high-resolution electrospray ionization mass spectroscopy (see Supporting Information).

First, the absorption and fluorescence properties of **1** and **2** in solution were examined. Compound **1** in the mixture of chloroform and methanol (1:1, v/v) exhibited peaks at 464 nm ($\epsilon = 3.9 \times 10^4$ L mol^{-1} cm^{-1}), 440 nm ($\epsilon = 3.7 \times 10^4$ L mol^{-1} cm^{-1}), and 273 nm ($\epsilon = 1.3 \times 10^5$ L mol^{-1} cm^{-1}) in the absorption spectrum (**Figure** 2a, left). In the emission spectrum, the solution exhibited two peaks, at 478 and 509 nm, and one shoulder at ≈540 nm, indicating a vibronic structure (Figure 2a, right). These spectral features are typical of 9,10-bis(phenylethynyl)anthracene luminophores in the monomeric state in solution.[35–37,69,70] The TEG chains allowed **2** to be soluble in more polar solvents and slightly changed its photophysical properties because of their electron-donating nature. The absorption spectrum of **2** in methanol exhibited peaks at 478 nm ($\epsilon = 5.4 \times 10^4$ L mol^{-1} cm^{-1}), 450 nm ($\epsilon = 4.4 \times 10^4$ L mol^{-1} cm^{-1}), and 275 nm ($\epsilon = 1.2 \times 10^5$ L mol^{-1} cm^{-1}) (Figure 2b, left). The highest emission peak was observed at 492 nm, which was red-shifted compared with that of **1** in solution (Figure 2b, right). Amphiphiles **1** and **2** showed good quantum yields: 0.94 in a mixture of chloroform and methanol (1:1, v/v) and 0.84 in methanol, respectively. Additionally, a monomer emission lifetime of 3.0 ns was calculated from the emission decay profiles recorded for the diluted solutions of **1** and **2** (Figure S1, Supporting Information).

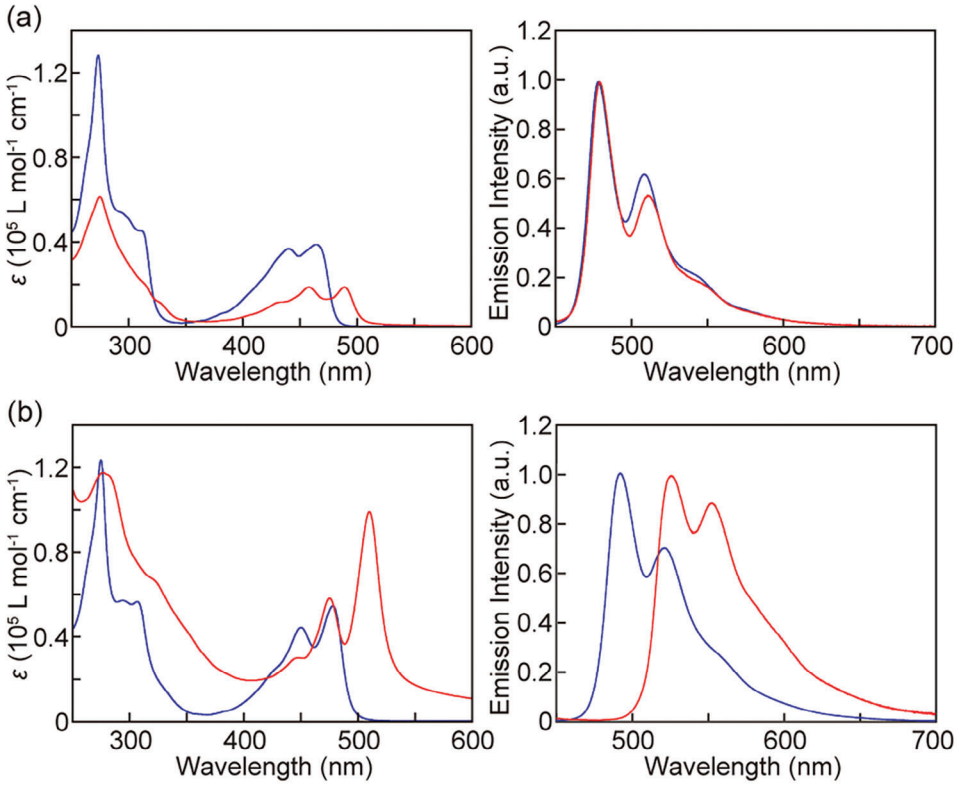

Figure 2. Absorption (left) and photoluminescence (right) spectra of a) amphiphile **1** in chloroform/methanol (1:1 v/v, blue line; 11.5:1 v/v, red line) and b) amphiphile **2** in methanol (blue line) and in water/methanol (7:3 v/v, red line). c = 1.0×10^{-5} M. The photoluminescence spectra were recorded with an excitation light of 400 nm.

Changing the solvent polarity altered the absorption spectra of **1** and **2** in solution. Increasing the ratio of chloroform resulted in the precipitation of compound **1** and redshift of the absorption band between 400 and 500 nm with peaks at 489 and 458 nm (Figure 2a, left). As partial precipitation occurred, the absorbance decreased. A more pronounced redshift was observed for **2** when water was added to the methanol solution. The absorption peak at the longest wavelength redshifted from 478 to 510 nm (Figure 2b, left). The baseline of the absorption spectrum was elevated because of light scattering from the aggregates. The redshifts in the absorption spectra of these amphiphiles suggest that the fluorophores formed *J*-aggregate-like arrangements.[71,72] The larger shift observed for **2** indicates that the fluorophore arrangements were different in **1** and **2**. The fluorescence spectrum of **2** also showed a large redshift when molecular aggregates were formed upon the addition of water, displaying peaks at 525 and 552 nm (Figure 2b, right). No significant redshift occurred in the fluorescence spectrum of **1**, presumably because numerous molecules in the monomeric state remained in the solution (Figure 2a, right). Notably, no excimer emission was observed for both solutions of **1** or **2** containing supramolecular assemblies.

Atomic force microscopy (AFM) and transmission electron microscopy (TEM) were used to elucidate the nature of the molecular assemblies of **1** and **2** in solution. The AFM images of the samples prepared by coating a chloroform/methanol (9:1, v/v) solution of **1** on mica (**Figure 3a** left; Figure S2, Supporting Information) show numerous fibers with a height of ≈1.5 nm. Some of the observed supramolecular fibers were over 1 µm in length. Supramolecular fibers were also observed in the TEM images of the sample prepared by coating the same solution onto an amorphous carbon film without staining (Figure 3a right; Figure S3, Supporting Information). The width of the supramolecular fiber was ≈5–6 nm, which corresponds to the length of **1**. The low height of the fibers observed in AFM images suggests that **1** was not stacked in a completely overlapping manner perpendicular to the direction of the fiber but rather in a tilted manner (Figure S4a, Supporting Information). 1D supramolecular fibers were also observed in the AFM images of the samples prepared from a water/methanol (7:3, v/v) solution of **2** (Figure 3b left; Figure S5, Supporting Information). Some fibers were attached to form a single strand, whereas others were branched. Longer and more flexible fibers were observed compared with the supramolecular fibers consisting of **1**. The height of the fibers was more distributed in the case of compound **2**. The TEM images also clarified that the fibers had the width of individual molecules (≈5 nm; Figure 3b right and Figure S6, Supporting Information). These results suggest that amphiphile **2** formed more hydrophilic supramolecular fibers (Figure S4b, Supporting Information) in a mixture of water and methanol owing to the TEG chains.

Infrared (IR) spectroscopic measurements were conducted to confirm that both amphiphiles formed intermolecular hydrogen bonds between the amide groups (**Figure 4**, top). Because the large absorption bands attributed to OH stretching mask peaks

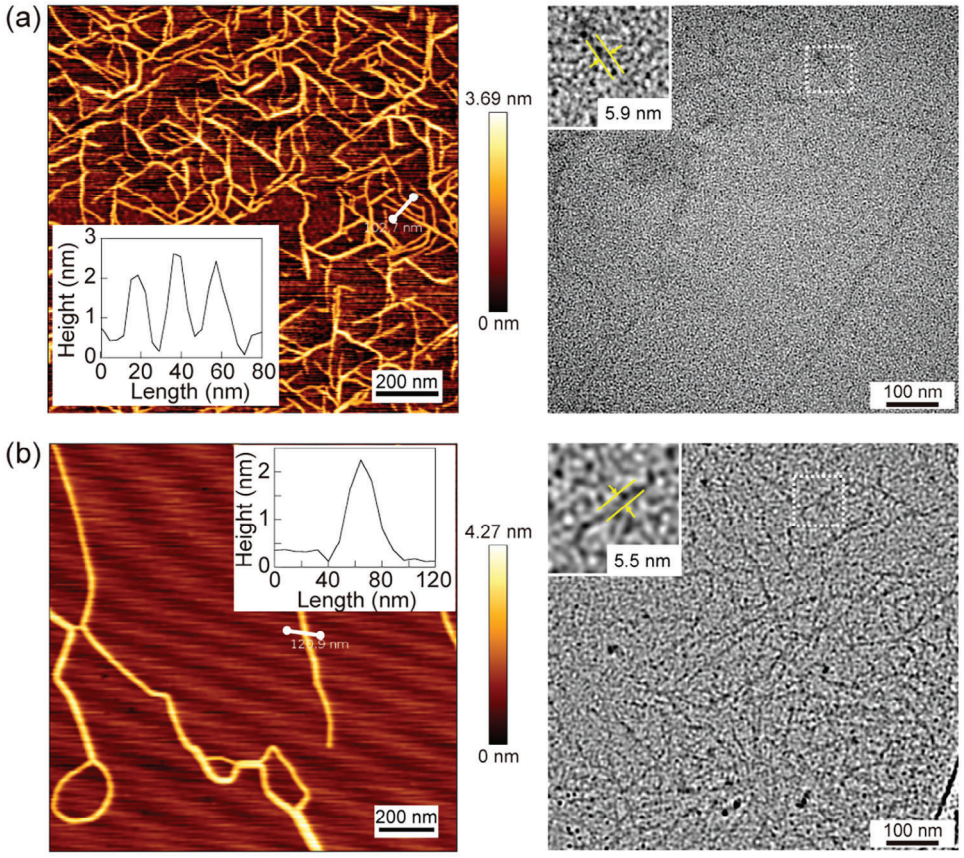

Figure 3. AFM (left) and TEM (right) images of supramolecular fibers consisting of a) **1** and b) **2**. The insets in the left panels show the height profiles of the supramolecular fibers. The insets in the right panels show magnified views of the areas enclosed by the dotted lines. The TEM images were taken without staining. Solutions of **1** in chloroform/methanol (9:1 v/v) and solutions of **2** in water/methanol (7:3 v/v) were used for sample preparation.

ascribed to N-H stretching of the amide groups, the C=O stretching of the amide groups was investigated for solid samples consisting of supramolecular fibers of **1** and **2**. The former sample was prepared by slow evaporation of a dichloroethane/methanol solution of **1**. Whereas the latter was obtained by removing most of the methanol from a methanol/water solution of compound **2** using an evaporator, followed by lyophilization. Amphiphiles **1** and **2** exhibited a peak at 1648 and 1640 cm^{-1}, respectively, indicating that the amide groups of both compounds formed intermolecular hydrogen bonds in the fibers, and no peaks corresponding to free amide groups were observed. The sharp peaks suggested the formation of uniform linear hydrogen bonds. Because the peak positions were different, the hydrogen bonding modes in the supramolecular fibers were also different, suggesting that the fluorophore arrangements are different from each other. These results are in good agreement with the fact that compound **2** exhibits a pronounced redshift of the absorption band, as shown in Figure 2.

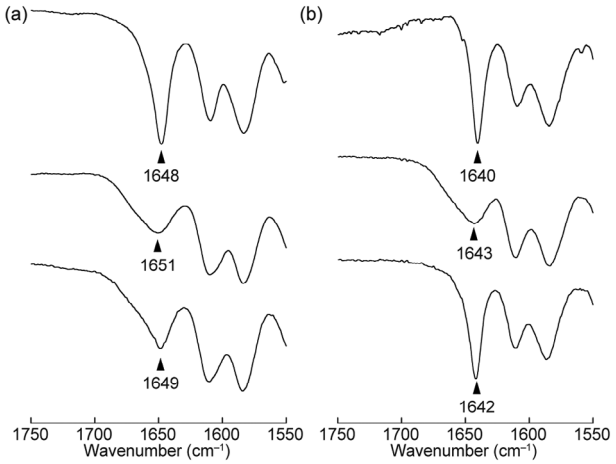

Figure 4. Partial IR spectra of a) **1** and b) **2** in the initial solid (top), ground states (middle), and dried films after the addition of water to ground samples (bottom).

The highest occupied molecular orbital (HOMO) and lowest unoccupied molecular orbital (LUMO) pictures and transition dipole moments for model compounds identical to the central molecular structures of **1** and **2** were calculated (Figures S7 and S8, Supporting Information). The HOMO and LUMO of both models lay primarily in the anthracene group. Both transition dipole moments were slightly tilted from the long axis of 9,10-bis(phenylethynyl)anthracene. No clear differences were observed in the HOMO and LUMO pictures and transition dipole moments between the models of **1** and **2**, indicating that the influence of the methoxy groups is negligible. Given that the

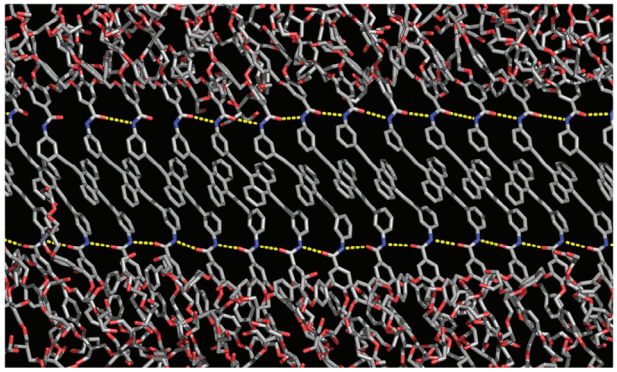

Figure 5. MD simulation snapshot of amphiphile **1** after 100 ns of equilibration run. Solvent molecules are not shown for clarity. Yellow dotted lines represent intermolecular hydrogen bonds between amide groups.

two amphiphiles form supramolecular fibers via linear hydrogen bonding, the stable dimer structures were optimized so that the carbonyl groups of the amide face toward and outward from the anthracene group (Figure S9, Supporting Information). Considering the direction of the dipole moments, both calculated arrangements of the luminophores result in a redshift of the absorption bands of **1** and **2** when the supramolecular fibers form as conventional *J*-aggregates show.

Molecular dynamics (MD) simulations were performed to investigate the molecular arrangement of the supramolecular fibers of **1**. MD simulation with the initial structure of the dimer revealed that the carbonyl groups of the amide facing the anthracene group (Figures S9a and S10a, Supporting Information) became a uniform linear supramolecular fiber (**Figure 5** and Figure S11, Supporting Information). The average height and width of the assembly fiber were estimated to be ≈1.8 and 5 nm, respectively; these values are consistent with those observed in the AFM and TEM images (Figure 3a). Additionally, the direction of the continuously connected intermolecular hydrogen bonds in the amide groups was parallel to the elongation direction of the fibers. The distances of the anthracene groups between neighboring molecules were found to be 0.45–0.5 nm, and fully overlapped π-stackings were not observed, suggesting that the molecules formed a *J*-aggregate-like arrangement. By contrast, the molecular assembly obtained from the MD simulation with the initial structure composed of the other type of dimer (Figures S9b and S10b, Supporting Information) indicated that the amide groups between neighboring molecules did not stably form linear hydrogen bonds, and the molecular arrangement was nonuniform (Figure S12, Supporting Information). The height of the molecular assembly exceeded 2.5 nm and its width was less than 3.5 nm. These values are distinct from those obtained from the experimental results (Figure 3a). Amphiphile **2** also formed supramolecular fibers, with an arrangement of amide groups similar to that in **1**. The introduced TEG chains would alter the thermodynamically stable molecular arrangement, which led to differences in the photophysical properties (Figure 2) and peaks corresponding to the C=O bonds in the infrared spectra (Figure 4, top).

Next, the mechanochromic luminescence of the supramolecular fibers and their response upon the addition of water were investigated (**Figure 6**). Neither of the supramolecular fibers were soluble in water. Green fluorescence was observed in the solid sample of the supramolecular fiber composed of **1** under excitation at 365 nm, whereas amphiphile **2** in fibers exhibited yellow-green fluorescence. When mechanically ground, their fluorescent colors turned yellow and orange, respectively. The grinding performed here is very straightforward. After placing a solid sample of **1** or **2** on a glass substrate, uniform grinding is performed with a metal spatula, requiring no special equipment. The entire sample should be thoroughly ground to properly induce the conversion of the molecular assemblies, which will be discussed later. Just pressing the solid sample results in little change in the photoluminescence properties. Unexpectedly, the responses of the ground samples significantly differed after the addition of water. The yellow emission of ground **1** was retained even after dissolution in water. By contrast, the emission color of **2** changed from orange to green. The orange photoluminescence obtained by grinding dry amphiphile **2** was not observed when compound **2** was wetted and ground directly.

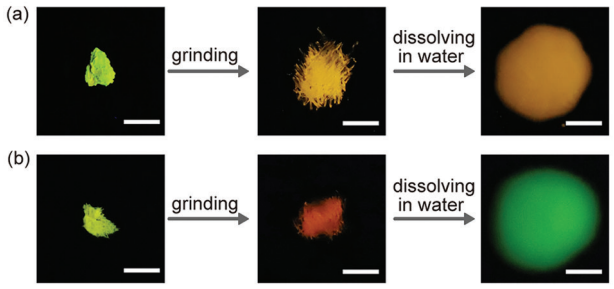

Figure 6. External Stimuli-responsive luminescence of amphiphiles a) **1** and b) **2**. Scale bar: 5 mm. All photos were recorded with an excitation light of 365 nm under dark conditions.

Fluorescence spectroscopy was performed to confirm the emission color changes upon grinding and subsequent addition of water (**Figure 7**). The initial solid supramolecular fibers of **1** and **2** displayed peaks at 529 and 552 nm, respectively, in addition to shoulders due to their vibronic structure. Although the emission intensity of the spectra at shorter wavelengths decreased because of self-absorption, monomer-like emission, similar to that recorded for solutions containing supramolecular fibers, was observed for both initial solids. After grinding, both emission spectra exhibited significant redshifts and became broad and structureless (Figure 7). These spectral features

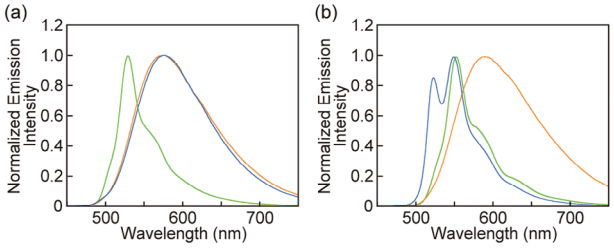

Figure 7. Photoluminescence spectra of a) **1** and b) **2** in the initial solid state (green), in the ground states (yellow), and in the water solution of ground samples (blue). All spectra were recorded with an excitation of 385 nm.

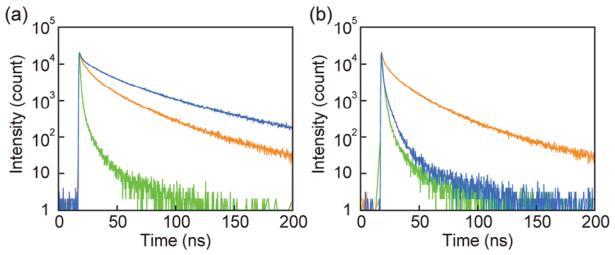

Figure 8. Emission decay profiles of a) **1** and b) **2** in the initial solid state (green), in the ground states (yellow), and in the water solution of ground samples (blue). The decay profiles of **1** were monitored at 565 nm (yellow and blue lines) and 535 nm (green line). The decay profiles of **2** were monitored at 600 nm (yellow line) and 560 nm (green and blue lines). All profiles were recorded with excitation light of 405 nm.

indicate that the fluorophores formed excimers in the ground samples. Similar static excimers were reported for several 9,10-bis(phenylethynyl)anthracene derivatives.[35–37] Furthermore, the addition of water to ground **1** did not significantly change the fluorescence spectrum, indicating that the excimers were well maintained. Therefore, compound **1** forms molecular assemblies different from those of the initial supramolecular fibers in water. The assembly of the luminophore in water was confirmed by the absorption spectroscopic measurements (Figure S13a, Supporting Information). The absorption spectrum of the aqueous solution of ground **1** is unambiguously red-shifted compared to that of **1** in chloroform/methanol (1:1 v/v) (Figure 2a). These results indicate that the fluorophores in water are arranged differently from those in the supramolecular fibers (Figure S4a, Supporting Information). By contrast, in the case of **2**, the addition of water caused a large blueshift in the fluorescence spectrum, with peaks observed at 523 and 549 nm (Figure 7b). This fluorescence spectrum was similar to that of the water/methanol solution in which the supramolecular fiber forms, thus suggesting that the excimer of the luminophore in **2** disappeared and the molecular assembly of the initial supramolecular fiber recovered. Indeed, the absorption spectrum of ground **2** in water was similar to that of the supramolecular fibers in a water/methanol solution (Figure S13b, Supporting Information), except for the unambiguous light-scattering effect. Ground **2** solved in the mixture of water/methanol (7:3 v/v) also shows almost the same absorption spectral shape between 400 and 550 nm as that of the initial supramolecular fibers in the same solvent mixture. In addition to dissolution in water, exposure to water vapor also induces recovery. Exposure of ground **2** to water vapor for 18 h shows a fluorescence maximum at almost the same wavelength as the water solution of ground **2** (Figure S14, Supporting Information).

To gain further insights into the external stimulus-induced changes in the fluorescence of both amphiphiles, fluorescence lifetime measurements were performed (**Figure 8**; Table S1, Supporting Information). All decay profiles recorded for the solid samples and water solutions of **1** and **2** were fitted with a triexponential decay function. The initial solid states of **1** and **2** forming supramolecular fibers showed emission lifetimes between 0.4 and 8.7 ns. After grinding, fluorescence decay became slow for both compounds. Longer lifetimes of 43 and 42 ns were obtained for ground **1** and **2** in the solid state, corresponding to the excimer emission lifetime. Longer lifetimes have also been reported for the excimers of 9,10-bis(phenylethynyl)anthracene derivatives.[35–37] A further slower decay was recorded after dissolving ground **1** in water, and the longest lifetime of 60 ns was obtained. By contrast, the water solution of ground **2** displayed a decay profile similar to that of **2** in the initial samples. The data obtained from these time-resolved fluorescence measurements support our speculation that the excimer-forming arrangement of luminophores after the grinding of **1** was retained upon the addition of water, whereas the initial supramolecular fiber arrangement recovered for **2** despite the significantly improved water solubility of **2**.

Mechanical grinding and subsequent dissolution in water affected the hydrogen bonding modes of **1** and **2**. As shown in Figure 4, peaks corresponding to the C=O stretching of amide groups in **1** and **2** appeared at 1651 and 1643 cm^{-1} after grinding in the solid states, respectively. Therefore, almost all amide groups were still involved in the formation of intermolecular hydrogen bonds. However, the broad peaks suggest that the mechanical grinding interfered with the linearly formed hydrogen bonds. After the addition of water to grounds **1** and **2**, thin films were prepared by the evaporation of water under ambient conditions and were subjected to infrared measurements (Figure 4, bottom). The broad peak ascribed to C=O stretching was still observed for **1**, indicating that the disordered structures induced by grinding remained after the addition of water. Conversely, compound **2** exhibits a sharp peak similar to that of the initial supramolecular fibers. This result also implies that the addition of water recovers the initial supramolecular fibers of **2**.

AFM and TEM observations were performed on **1** and **2** to clarify their assembled structures after the ground samples were dissolved in water. Several spherical structures with heights of ≈4 nm were observed in the AFM images of the sample prepared from the aqueous solution of ground **1** (**Figure 9**a left; Figure S15, Supporting Information). The TEM images also showed numerous spheres with diameters between 1 and 3 nm (Figure 9a right; Figure S16, Supporting Information). These results indicate that compound **1** formed micellar assemblies (Figure S17, Supporting Information) after mechanical grinding and dissolution in water. The micelles are assumed to be two-dimensionally assembled into disk-like structures in the AFM images, which is why a large difference in diameters was observed between the AFM and TEM images. In the micelles, as excimer fluorescence was observed, the luminophores formed π-stacked structures. Given that the length between amide groups involved in hydrogen bonds is generally longer than the distance between aromatic groups forming π-stacking, a disordered hydrogen-bonding mode was adopted, thus resulting in the broadening of the C=O stretching peak observed in the IR spectrum (Figure 4). Similar micellar structures have been reported in previous studies of dumbbell-shaped amphiphiles.[50] The micelle-like structure was assumed to form when ground in the solid phase because the emission spectra of ground **1** and water solution of micelles are almost identical. Small changes in the molecular arrangement should occur upon dissolution in water because the emission decay becomes slower (Figure 8a) and the shape of the peak ascribed to C=O stretching in the IR spectrum changes slightly (Figure 4a). Because the dendritic structures were not well-packed, the length of the micelles in the TEM image became less than the molecular length.

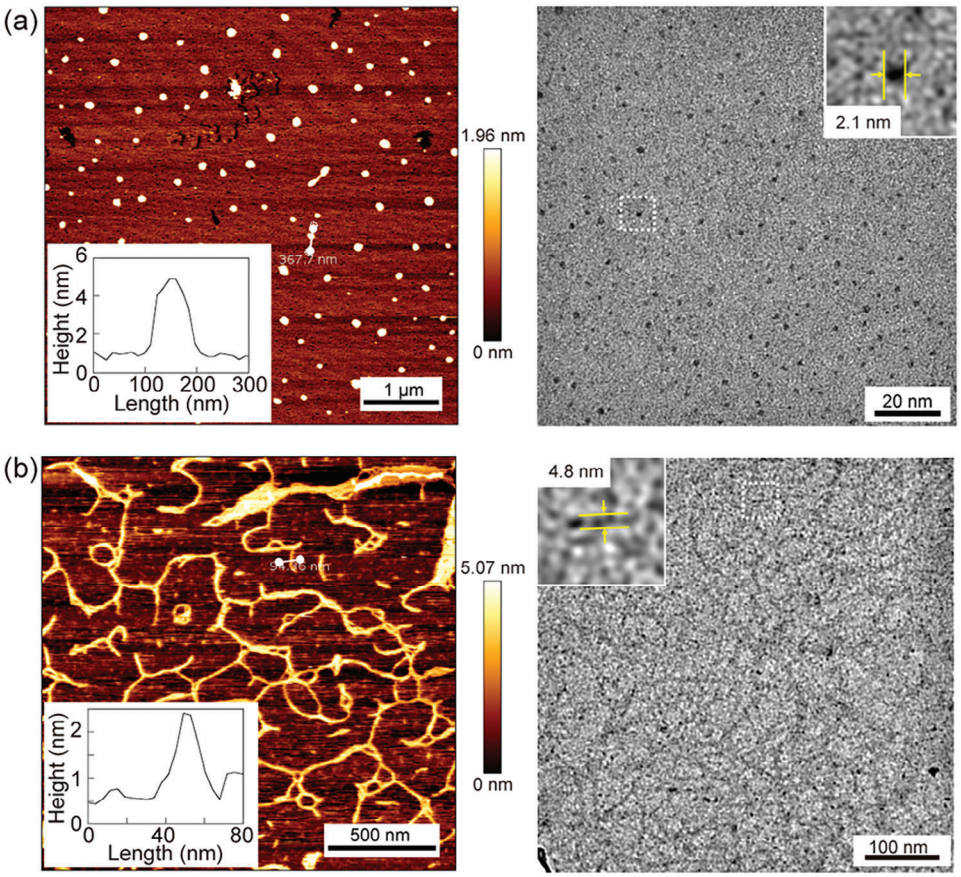

Figure 9. AFM (left) and TEM (right) images of a) micelles consisting of **1** and b) fragmented supramolecular fibers of **2**. The insets in the left panels show the height profiles of the micelles or supramolecular fibers. The insets in the right panels show magnified views of the areas enclosed by the dotted lines. The TEM images were taken without staining. The water solutions of ground **1** or **2** were used for both sample preparation.

In contrast to the micelles of **1**, fragmented fibrous molecular assemblies with a height of ≈2 nm were observed in the AFM images of the aqueous solution of ground **2** (Figure 9b left; Figure S18, Supporting Information). The lengths of the fibers became shorter than those of the initial supramolecular fibers. The TEM images also showed numerous fibers with a width of 5 nm (Figure 9b right; Figure S19, Supporting Information). These height and width values coincide with those of the initial supramolecular fibers consisting of **2** (Figure 3b; Figures S5 and S6, Supporting Information). Considering the recovery of the fluorescence properties and the sharp peak attributed to C=O stretching in the IR spectrum, the initial molecular assembly of **2** should recover by the addition of water after grinding, although fragmentation occurred.

The proposed changes in the molecular assemblies of **1** and **2** in response to mechanical stimuli and the addition of water are shown in Figure 1b. Initially, the amide groups of **1** and **2** formed linear 1D hydrogen bonds. The fluorophores were placed in *J*-aggregate-like arrangements showing monomer-like fluorescence. In the assembled structures, hydrophilic dendrons do not prevent the formation of supramolecular fibers at the micrometer scale. In the supramolecular fiber of **1**, the arrays of highly hydrophobic fluorophores are uncovered. Therefore, the hydrophilicity was not high, and supramolecular fibers formed in the chloroform-methanol mixture. By contrast, in the case of **2**, as the arrays of hydrophobic fluorophores were covered with TEG chains, the supramolecular fibers were highly hydrophilic and formed in the water-methanol mixture. When amphiphile **1** in the solid consisting of the supramolecular fibers was ground, the supramolecular fibers were converted to micellar assemblies in which the amide groups no longer formed the linear hydrogen bond, and fluorophores formed π-stacked structures. Consequently, ground **1** exhibited excimer emissions. In this luminophore arrangement, moderately bulky hydrophilic dendrons prevented the compounds from forming 1D linear assemblies. Compared with the initial *J*-aggregate-like arrangement of **1**, the fragmented array of the hydrophobic fluorophores in the micelles of **1** was surrounded by hydrophilic dendrons. Therefore, after the addition of water, the micellar assemblies were retained because they were more thermodynamically stable in water. This is the first example of supramolecular fibers being converted to micelles by mechanical stimuli, concomitant with emission color changes. The transition to micelles endowed **1** with water solubility, although the initial supramolecular fibers were insoluble in water. Owing to the molecular structural similarity between **1** and **2**, amphiphile **2** is also expected to form micellar structures after grinding, resulting in excimer emission. This assumption is also supported by the fact that micellar

structures were observed in the AFM image taken for the sample prepared with a water/methanol solution (3:7, v/v) of ground **2** (Figure S20, Supporting Information). In the case of **2**, the fragmented supramolecular fibers were more stable than micellar assemblies in water because the hydrophobic arrays of the luminophores were covered with hydrophilic TEG groups. Therefore, the addition of water results in the conversion of micellar assemblies in the ground solid to fragmented supramolecular fibers in water, thus resulting in the recovery of the initial emission properties. Consequently, the fragmentation of the supramolecular fibers allowed them to dissolve in water. We assume that the significant difference in water solubility between the initial supramolecular fibers of **2** and the fragmented fibers after grinding is also ascribed to the inter-fiber interactions. Before grinding, amphiphile **2** forms long supramolecular fibers and forms fiber bundles in which strong inter-fiber interactions occur. Therefore, amphiphile **2** cannot be dispersed in water. After grinding and the addition of water, the original molecular arrangements are restored. However, since the fragmented fibers are separated from each other and cannot form fiber bundles by being surrounded by water molecules, we speculate that the fragmented fibers may dissolve in water.

3. Conclusion

In summary, mechanochromic luminescent supramolecular fibers consisting of dumbbell-shaped amphiphiles **1** and **2** were successfully developed. In the initial supramolecular fibers, the luminophore 9,10-bis(phenylethynyl)anthracene formed *J*-aggregate-like arrangements via linear hydrogen bonding between the amide groups. Because the hydrogen-bonding modes in the fibers of **1** and **2** were slightly different, compound **2** exhibited a more pronounced redshift in the absorption spectrum. Both the compounds in the water-insoluble fibers became water-soluble after grinding in the solid state. When ground, the uniform hydrogen bonds were disturbed, and linear supramolecular fibers were converted into micellar assemblies. In force-induced molecular assembled structures, the luminophores formed excimers, thus leading to a significant redshift of the emission spectra. As the micellar structures were favorable for **1** in water, the grinding-induced yellow fluorescence was retained after the addition of water. Hydrophilic TEG chains introduced to the hydrophobic fluorophores of **2** stabilized the fragmented supramolecular fibers in water, thus resulting in the recovery of the initial fluorescence properties upon water addition.

Mechanochromic fluorescent supramolecular fibers have a significant advantage over conventional crystalline materials in that they can be dispersed and supported on the surface of the material where the force is needed to be detected. Furthermore, as these fibers are only one molecule wide and uniform, the force required to induce a fluorescent color change is constant and highly small. In the previous study on mechanochromic fluorescent micelles in which fluorophore is π-stacked to exhibit excimer emission, fluorescence color change was realized only when all the arrangements of the fluorophores in the micelle were changed by force to ensure that no excimer sites existed. However, in supramolecular fibers, if only one excimer site is created by mechanical stimuli, energy transfer from the fluorophore occurs in the monomeric state, thus resulting in good sensitivity to forces. Furthermore, compared with mechanophores, which detect forces at the single-molecule level, supramolecular fibers are advantageous in that they can detect forces at the mesoscale without the need to introduce them into polymers or other materials. Currently, we are attempting to establish methods to quantitatively evaluate mechanoresponsive luminescence for supramolecular fibers under conditions in which they are dispersed and supported by other materials.

Supporting Information

Supporting Information is available from the Wiley Online Library or from the author.

Acknowledgements

The authors thank the Materials Analysis Division, Open Facility Center, Tokyo Institute of Technology, for the HRMS measurements. This work was supported by JSPS KAKENHI (grant numbers JP23H04878, JP23H04874, and JP23H04879) in a Grant-in-Aid for Transformative Research Areas "Materials Science of Meso-Hierarchy." This study was also supported by a Grant-in-Aid for Scientific Research on Innovative Areas "Aquatic Functional Materials" (grant numbers JP19H05718 and JP22H04531). Additionally, it was supported by JSPS KAKENHI (grant number JP16K17885), JST CREST JPMJCR20B2, and the JGC-S SCHOLARSHIP FOUNDATION. Furthermore, this study was supported in part by the Multidisciplinary Cooperative Research Program of the Center for Computational Sciences at the University of Tsukuba. Some of the computations were performed using computer facilities at the Research Institute for Information Technology, Kyushu University, and the Research Center for Computational Science, Okazaki, Japan (Project: 23-IMS-C038 and 23-IMS-C109).

Conflict of Interest

The authors declare no conflict of interest.

Data Availability Statement

The data that support the findings of this study are available in the supplementary material of this article.

Keywords

amphiphiles, grinding-induced water solubility, *J*-aggregation, mechanochromic luminescence, micelles, supramolecular polymers

Received: January 3, 2024
Revised: February 28, 2024
Published online: March 10, 2024

[1] Y. Sagara, S. Yamane, M. Mitani, C. Weder, T. Kato, *Adv. Mater.* **2016**, *28*, 1073.
[2] Y. Sagara, T. Kato, *Nat. Chem.* **2009**, *1*, 605.
[3] Z. Chi, X. Zhang, B. Xu, X. Zhou, C. Ma, Y. Zhang, S. Liu, J. Xu, *Chem. Soc. Rev.* **2012**, *41*, 3878.
[4] Z. Ma, Z. Wang, M. Teng, Z. Xu, X. Jia, *ChemPhysChem* **2015**, *16*, 1811.
[5] S. Ito, *J. Photochem. Photobiol.* **2022**, *51*, 100481.

[6] S. Ito, *CrystEngComm* **2022**, *24*, 1112.
[7] S. Ito, *Chem. Lett.* **2021**, *50*, 649.
[8] Y. Sagara, T. Mutai, I. Yoshikawa, K. Araki, *J. Am. Chem. Soc.* **2007**, *129*, 1520.
[9] J. Kunzelman, M. Kinami, B. R. Crenshaw, J. D. Protasiewicz, C. Weder, *Adv. Mater.* **2008**, *20*, 119.
[10] Y. Sagara, T. Kato, *Angew. Chem. Int. Ed.* **2008**, *47*, 5175.
[11] Y. Ooyama, Y. Kagawa, H. Fukuoka, G. Ito, Y. Harima, *Eur. J. Org. Chem.* **2009**, 5321.
[12] S.-J. Yoon, J. W. Chung, J. Gierschner, K. S. Kim, M.-G. Choi, D. Kim, S. Y. Park, *J. Am. Chem. Soc.* **2010**, *132*, 13675.
[13] Y. Ooyama, G. Ito, H. Fukuoka, T. Nagano, Y. Kagawa, I. Imae, K. Komaguchi, Y. Harima, *Tetrahedron* **2010**, *66*, 7268.
[14] Y. Sagara, T. Kato, *Angew. Chem. Int. Ed.* **2011**, *50*, 9128.
[15] X. Luo, J. Li, C. Li, L. Heng, Y. Q. Dong, Z. Liu, Z. Bo, B. Z. Tang, *Adv. Mater.* **2011**, *23*, 3261.
[16] H. Li, X. Zhang, Z. Chi, B. Xu, W. Zhou, S. Liu, Y. Zhang, J. Xu, *Org. Lett.* **2011**, *13*, 556.
[17] M. J. Teng, X. R. Jia, X. F. Chen, Y. Wei, *Angew. Chem. Int. Ed.* **2012**, *51*, 6398.
[18] M. S. Kwon, J. Gierschner, S. J. Yoon, S. Y. Park, *Adv. Mater.* **2012**, *24*, 5487.
[19] X. Gu, J. Yao, G. Zhang, Y. Yan, C. Zhang, Q. Peng, Q. Liao, Y. Wu, Z. Xu, Y. Zhao, H. Fu, D. Zhang, *Adv. Funct. Mater.* **2012**, *22*, 4862.
[20] Y. Dong, B. Xu, J. Zhang, X. Tan, L. Wang, J. Chen, H. Lv, S. Wen, B. Li, L. Ye, B. Zou, W. Tian, *Angew. Chem. Int. Ed.* **2012**, *51*, 10782.
[21] N. Mizoshita, T. Tani, S. Inagaki, *Adv. Mater.* **2012**, *24*, 3350.
[22] J. Wang, J. Mei, R. Hu, J. Z. Sun, A. Qin, B. Z. Tang, *J. Am. Chem. Soc.* **2012**, *134*, 9956.
[23] K. Nagura, S. Saito, H. Yusa, H. Yamawaki, H. Fujihisa, H. Sato, Y. Shimoikeda, S. Yamaguchi, *J. Am. Chem. Soc.* **2013**, *135*, 10322.
[24] W. Z. Yuan, Y. Tan, Y. Gong, P. Lu, J. W. Lam, X. Y. Shen, C. Feng, H. H. Sung, Y. Lu, I. D. Williams, J. Z. Sun, Y. Zhang, B. Z. Tang, *Adv. Mater.* **2013**, *25*, 2837.
[25] M.-S. Yuan, D.-E. Wang, P. Xue, W. Wang, J.-C. Wang, Q. Tu, Z. Liu, Y. Liu, Y. Zhang, J. Wang, *Chem. Mater.* **2014**, *26*, 2467.
[26] H. J. Kim, D. R. Whang, J. Gierschner, C. H. Lee, S. Y. Park, *Angew. Chem. Int. Ed.* **2015**, *54*, 4330.
[27] L. Wang, K. Wang, B. Zou, K. Ye, H. Zhang, Y. Wang, *Adv. Mater.* **2015**, *27*, 2918.
[28] Y. Sagara, Y. C. Simon, N. Tamaoki, C. Weder, *Chem. Commun.* **2016**, *52*, 5694.
[29] Z. Ma, Z. Wang, X. Meng, Z. Ma, Z. Xu, Y. Ma, X. Jia, *Angew. Chem. Int. Ed.* **2016**, *55*, 519.
[30] S. K. Park, I. Cho, J. Gierschner, J. H. Kim, J. H. Kim, J. E. Kwon, O. K. Kwon, D. R. Whang, J.-H. Park, B.-K. An, S. Y. Park, *Angew. Chem. Int. Ed.* **2016**, *55*, 203.
[31] M. Okazaki, Y. Takeda, P. Data, P. Pander, H. Higginbotham, A. P. Monkman, S. Minakata, *Chem. Sci.* **2017**, *8*, 2677.
[32] Y. Sagara, K. Kubo, T. Nakamura, N. Tamaoki, C. Weder, *Chem. Mater.* **2017**, *29*, 1273.
[33] Y. Sagara, C. Weder, N. Tamaoki, *Chem. Mater.* **2017**, *29*, 6145.
[34] A. Lavrenova, D. W. Balkenende, Y. Sagara, S. Schrettl, Y. C. Simon, C. Weder, *J. Am. Chem. Soc.* **2017**, *139*, 4302.
[35] Y. Sagara, K. Takahashi, T. Nakamura, N. Tamaoki, *Chem. Asian J.* **2020**, *15*, 478.
[36] Y. Sagara, K. Takahashi, T. Nakamura, N. Tamaoki, *J. Mater. Chem. C* **2020**, *8*, 10039.
[37] Y. Sagara, K. Takahashi, A. Seki, T. Muramatsu, T. Nakamura, N. Tamaoki, *J. Mater. Chem. C* **2021**, *9*, 1671.
[38] H. Ito, T. Saito, N. Oshima, N. Kitamura, S. Ishizaka, Y. Hinatsu, M. Wakeshima, M. Kato, K. Tsuge, M. Sawamura, *J. Am. Chem. Soc.* **2008**, *130*, 10044.
[39] V. N. Kozhevnikov, B. Donnio, D. W. Bruce, *Angew. Chem. Int. Ed.* **2008**, *47*, 6286.
[40] H. Ito, M. Muromoto, S. Kurenuma, S. Ishizaka, N. Kitamura, H. Sato, T. Seki, *Nat. Commun.* **2013**, *4*, 2009.
[41] Q. Benito, X. F. Le Goff, S. Maron, A. Fargues, A. Garcia, C. Martineau, F. Taulelle, S. Kahlal, T. Gacoin, J. P. Boilot, S. Perruchas, *J. Am. Chem. Soc.* **2014**, *136*, 11311.
[42] H. Sun, S. Liu, W. Lin, K. Y. Zhang, W. Lv, X. Huang, F. Huo, H. Yang, G. Jenkins, Q. Zhao, W. Huang, *Nat. Commun.* **2014**, *5*, 3601.
[43] T. Seki, Y. Takamatsu, H. Ito, *J. Am. Chem. Soc.* **2016**, *138*, 6252.
[44] B. Huitorel, Q. Benito, A. Fargues, A. Garcia, T. Gacoin, J.-P. Boilot, S. Perruchas, F. Camerel, *Chem. Mater.* **2016**, *28*, 8190.
[45] T. Seki, N. Tokodai, S. Omagari, T. Nakanishi, Y. Hasegawa, T. Iwasa, T. Taketsugu, H. Ito, *J. Am. Chem. Soc.* **2017**, *139*, 6514.
[46] M. Jin, T. Seki, H. Ito, *J. Am. Chem. Soc.* **2017**, *139*, 7452.
[47] Y. Ren, W. H. Kan, V. Thangadurai, T. Baumgartner, *Angew. Chem. Int. Ed.* **2012**, *51*, 3964.
[48] Y. Sagara, T. Komatsu, T. Ueno, K. Hanaoka, T. Kato, T. Nagano, *Adv. Funct. Mater.* **2013**, *23*, 5277.
[49] S. Yagai, S. Okamura, Y. Nakano, M. Yamauchi, K. Kishikawa, T. Karatsu, A. Kitamura, A. Ueno, D. Kuzuhara, H. Yamada, T. Seki, H. Ito, *Nat. Commun.* **2014**, *5*, 4013.
[50] Y. Sagara, T. Komatsu, T. Ueno, K. Hanaoka, T. Kato, T. Nagano, *J. Am. Chem. Soc.* **2014**, *136*, 4273.
[51] Y. Sagara, T. Komatsu, T. Terai, T. Ueno, K. Hanaoka, T. Kato, T. Nagano, *Chem. Eur. J.* **2014**, *20*, 10397.
[52] C. Liang, M. Li, Y. Chen, *ACS Appl. Mater. Interfaces* **2021**, *13*, 20698.
[53] Y. Chen, A. Li, X. Li, L. Tu, Y. Xie, S. Xu, Z. Li, *Adv. Mater.* **2023**, *35*, 2211917.
[54] J. H. Ryu, D. J. Hong, M. Lee, *Chem. Commun.* **2008**, 1043.
[55] X. Zhang, S. Rehm, M. M. Safont-Sempere, F. Würthner, *Nat. Chem.* **2009**, *1*, 623.
[56] Y. B. Lim, K. S. Moon, M. Lee, *Chem. Soc. Rev.* **2009**, *38*, 925.
[57] T. Heek, C. Fasting, C. Rest, X. Zhang, F. Wurthner, R. Haag, *Chem. Commun.* **2010**, *46*, 1884.
[58] H.-J. Kim, T. Kim, M. Lee, *Acc. Chem. Res.* **2011**, *44*, 72.
[59] B. N. Thota, L. H. Urner, R. Haag, *Chem. Rev.* **2016**, *116*, 2079.
[60] Y. Sagara, M. Karman, E. Verde-Sesto, K. Matsuo, Y. Kim, N. Tamaoki, C. Weder, *J. Am. Chem. Soc.* **2018**, *140*, 1584.
[61] Y. Sagara, M. Karman, A. Seki, M. Pannipara, N. Tamaoki, C. Weder, *ACS Cent. Sci.* **2019**, *5*, 874.
[62] Y. Sagara, H. Traeger, J. Li, Y. Okado, S. Schrettl, N. Tamaoki, C. Weder, *J. Am. Chem. Soc.* **2021**, *143*, 5519.
[63] T. Muramatsu, Y. Okado, H. Traeger, S. Schrettl, N. Tamaoki, C. Weder, Y. Sagara, *J. Am. Chem. Soc.* **2021**, *143*, 9884.
[64] H. Traeger, Y. Sagara, D. J. Kiebala, S. Schrettl, C. Weder, *Angew. Chem. Int. Ed.* **2021**, *60*, 16191.
[65] S. Thazhathethil, T. Muramatsu, N. Tamaoki, C. Weder, Y. Sagara, *Angew. Chem. Int. Ed.* **2022**, *61*, 202209225.
[66] S. Shimizu, H. Yoshida, K. Mayumi, H. Ajiro, Y. Sagara, *Mater. Chem. Front.* **2023**, *7*, 4073.
[67] T. Muramatsu, S. Shimizu, J. M. Clough, C. Weder, Y. Sagara, *ACS Appl. Mater. Interfaces* **2023**, *15*, 8502.
[68] K. Hiratsuka, T. Muramatsu, T. Seki, C. Weder, G. Watanabe, Y. Sagara, *J. Mater. Chem. C* **2023**, *11*, 3949.
[69] M. Lübtow, I. Helmers, V. Stepanenko, R. Q. Albuquerque, T. B. Marder, G. Fernández, *Chem. Eur. J.* **2017**, *23*, 6198.
[70] M. Levitus, M. A. Garcia-Garibay, *J. Phys. Chem. A* **2000**, *104*, 8632.
[71] F. Würthner, T. E. Kaiser, C. R. Saha-Möller, *Angew. Chem. Int. Ed.* **2011**, *50*, 3376.
[72] T. E. Kaiser, V. Stepanenko, F. Würthner, *J. Am. Chem. Soc.* **2009**, *131*, 6719.